Journal of Nuclear Medicine, published on December 2, 2021 as doi:10.2967/jnumed.121.262831

Head-to-head comparison of ^{68}Ga-FAPI-46 and ^{18}F-FDG PET/CT for evaluation of head and neck squamous cell carcinoma: a single-center exploratory study

Chetsadaporn Promteangtrong[1*], Dheeratama Siripongsatian[1], Attapon Jantarato[1], Anchisa Kunawudhi[1], Peerapon Kiatkittikul[1], Sukanya Yaset[1], Natphimol Boonkawin[1], Chanisa Chotipanich[1]

[1]National Cyclotron and PET Centre, Chulabhorn Hospital, Chulabhorn Royal Academy, Bangkok, Thailand

*Correspondence to:

Chetsadaporn Promteangtrong, M.D.

National Cyclotron and PET Centre, Chulabhorn Royal Academy

906 Kamphaeng Phet 6 Rd., Lak Si, Bangkok 10210, Thailand

Tel: +66816286988; E-mail: chetsadaporn.pro@pccms.ac.th

Word count: 4611

Source of funding: None

Running short title: FAPI and FDG PET in HNSCC

ABSTRACT

^{68}Ga–conjugated fibroblast activation protein inhibitor (^{68}Ga-FAPI) has become an attractive agent for positron emission tomography (PET). This study aimed to compare ^{68}Ga-FAPI-46 PET/computed tomography (CT) with ^{18}F-fluorodeoxy-D-glucose (^{18}F-FDG) PET/CT for detecting primary cancer and metastatic lesions in patients with head and neck squamous cell carcinoma (HNSCC).

Methods: Twelve patients and twenty-eight patients with HNSCC underwent ^{68}Ga-FAPI-46 and ^{18}F-FDG PET/CT for initial staging and recurrence detection, respectively. Concordance and diagnostic accuracy of both tracers were analyzed. Semiquantitative parameters, including the maximum and mean of standardized uptake value (SUVmax and SUVmean) and tumor-to-background ratio (T/B) were compared. FAP expression tumor volume (FTV) and total lesion FAP expression (TLF) of ^{68}Ga-FAPI-46 were compared with metabolic tumor volume (MTV) and total lesion glycolysis (TLG) of ^{18}F-FDG, respectively. Differences between semiquantitative parameters were analyzed using paired t-tests.

Results: ^{68}Ga-FAPI -46 PET/CT was 83.3% and 96.4% concordant with ^{18}F-FDG PET/CT for initial staging and recurrence detection, respectively. Eighteen lesions had histopathological validation and both tracers displayed 100% sensitivity, 50% specificity, and 94.4% accuracy for lesion-based analysis. FTV was greater than MTV ($P < 0.05$), but no significant differences were observed for the other parameters.

Conclusion: ^{68}Ga-FAPI-46 PET/CT showed good concordance and comparable diagnostic performance compared with ^{18}F-FDG PET/CT for initial staging and recurrence detection in patients with HNSCC.

Key words: FAPI, FDG, PET/CT

INTRODUCTION

Head and neck squamous cell carcinoma (HNSCC) is the sixth most common carcinoma worldwide, with 890,000 new cases and 450,000 deaths reported in 2018 (*1*). The treatment of HNSCC depends on the anatomical site, tumor stage, and functional outcome. Early-stage cancers are treated with a single modality, such as surgery or radiotherapy alone; while locally advanced cancers require multimodal treatment, which is often a combination of surgery, radiotherapy, and chemotherapy. Therefore, accurate tumor staging is crucial for planning treatment strategies. ^{18}F-fluorodeoxy-D-glucose positron emission tomography/computed tomography (^{18}F-FDG PET/CT) is a widely accepted tool for imaging various cancers. However, ^{18}F-FDG PET/CT has some limitations when used for HNSCC. High glucose uptake is observed in several normal tissues, such as salivary glands, lymphoid tissues, and lymph nodes. Furthermore, false-positive uptake may occur in areas of peritumoral inflammation or after surgery and radiotherapy (*2*).

The tumor microenvironment in HNSCC is a mix of tumor and stromal cells, including endothelial cells, immune cells, and cancer-associated fibroblasts (CAFs). CAFs secrete a broad range of growth factors, cytokines, and chemokines that promote tumor growth, angiogenesis, and recruitment of immunosuppressive immune cells; thus, CAFs have a role in HNSCC invasion and progression (*3*). Fibroblast activation protein (FAP) is overexpressed by CAFs in several types of cancer, including HNSCC, with relatively low expression in normal tissue. Gallium-68 (^{68}Ga)–conjugated FAP inhibitor (FAPI), has been developed for targeting FAP and tumor stromal visualization (*4*). In previous studies, ^{68}Ga-FAPI-04 PET/CT showed a higher sensitivity than ^{18}F-FDG PET/CT in various types of cancers (5), and FAPI PET precisely delineated HNSCC for radiotherapy planning (*6*). The aim of this study was to conduct a head-to-head comparison of ^{68}Ga-FAPI-46 PET/CT and standard ^{18}F-FDG PET/CT imaging for detecting primary cancer and metastatic lesions in patients with HNSCC.

MATERIALS & METHODS

Study design

This was a single center exploratory comparative imaging study. The study was approved by the Human Research Ethics Committee of Chulabhorn Research Institute (study Registration number is TCTR20210902003, (https://www.thaiclinicaltrials.org/show/TCTR20210902003) and all subjects provided written informed consent. There was no external source of funding. Study protocol was provided as a supplement file.

Study Population

Potentially eligible HNSCC patients were recruited for enrolment in this study from August 2020 through May 2021. The inclusion criteria were as follows: (i) patients with pathologically confirmed HNSCC; (ii) patients who were > 18 years old; and (iii) patients who were scheduled for PET/CT with indication for initial staging or suspected recurrence. Exclusion criteria included (i) patients with fasting blood sugar > 150 mg/dL; (ii) patients who were pregnant or breast feeding; and (iii) patients who were unwilling to participate. The flowchart of the study design is presented in Figure 1.

Preparation of ^{68}Ga-FAPI-46

^{68}Ga-FAPI-46 was synthesized using the iTG ^{68}Ge/^{68}Ga generator and automated module (iQS-TS, ITM Medical Isotopes GmbH, Munich, Germany) and a good manufacturing practice-compliant process, as previously described (*7, 8*) with some modifications.

PET/CT Imaging

^{18}F-FDG and ^{68}Ga-FAPI-46 PET/CT were performed on separated days within a 2-week period. Patients fasted for 6 h prior to the ^{18}F-FDG PET/CT scanning, while no specific preparation was required on the day of ^{68}Ga-FAPI-46 PET/CT scanning. The plasma glucose level was determined prior to the ^{18}F-FDG PET/CT scan to ensure it was ≤ 150 mg/dL. The intravenous

injection dose was calculated according to the patient's weight in kg (2.59 MBq/kg for FDG; 2.0 MBq/kg for FAPI). After 60 min of intravenous administration, scanning were acquired from the vertex to the proximal thigh using a 64-slice Siemens/Biograph vision PET/CT scanner (Siemens Healthcare GmbH, Erlangen, Germany) in the three-dimensional mode with continuous bed motion method, speed of 1.6–1.8 mm/s. The matrix size was 440 x 440, and the reconstruction methods were True X and Time of Flight. The CT parameters were tube voltage of 120 kV, current of 25 mAs, and a slice thickness of 3.0 mm. ^{68}Ga-FAPI-46 PET/CT was performed for a comparative purpose without impacting on the final patients' management.

PET/CT Imaging Analysis

^{18}F-FDG and ^{68}Ga-FAPI-46 PET/CT scans were separately interpreted by three board-certified nuclear medicine physicians by consensus within 2 weeks apart. ^{18}F-FDG PET/CT were reviewed by D.S., P.K. and C.C. while ^{68}Ga-FAPI-46 PET/CT were reviewed by C.P., A.K. and C.C. The physicians were unaware of the clinical data at the time of review. PET, CT, and fused PET/CT images were viewed using the Syngo.via workstation (Siemens Healthcare GmbH).

Based on visual detection, an area of focal uptake higher than that of the surrounding background was considered positive. The lesion was categorized as primary tumor, nodal metastasis or distant metastasis. Nodal metastasis was classified according to location: neck, supraclavicular, mediastinum, axilla, and intra-abdominal sites. Brain, visceral organs in the chest and abdomen, bone, and soft tissue involvement were each classified as individual sites. Synchronous and second primary tumors were also analyzed. For initial staging, the clinical TNM stage of HNSCC was based on the eighth edition of the American Joint Committee on Cancer staging system (*9*).

Three-dimensional voxels of interest were drawn around the lesions and semiquantitative analysis was performed by the three designated physicians described above. The physicians adjusted the results to avoid false positive regions caused by normal physiological uptake. The

tumor region was delineated automatically using a standardized uptake value, which was 40% of the maximum standardized uptake value (SUVmax). The SUVmax, the mean standardized uptake value (SUVmean), and the tumor-to-background ratio (T/B) of the primary tumor and distant metastasis were recorded. T/B was determined by dividing SUVmax with SUVmean of the contralateral normal tissue. Metabolic tumor volume (MTV) and total lesion glycolysis (TLG) assessed by ^{18}F-FDG were compared with the equivalent values, naming FAP expression tumor volume (FTV) and total lesion FAP expression (TLF) assessed by ^{68}Ga-FAPI-46. The T/B was determined by dividing the tumor SUVmax by the SUVmean of the contralateral normal tissue. MTV and FTV were calculated by multiplying the number of voxels in the tumor region by voxel size. TLG and TLF were calculated by multiplying MTV or FTV with the corresponding SUVmean for each tumor volume. If multiple positive lesions occurred at a single metastatic site, the lesion with the highest activity was analyzed. For nodal metastasis, the SUVmax was calculated for each site.

Reference Standard

Histopathology served as the gold standard for diagnostic accuracy analysis. The reference standard used for non-biopsied lesions was the anatomical abnormality observed on CT or magnetic resonance imaging (MRI). An anatomical criterion for nodal metastasis was a cluster of at least 3 size-independent nodes at one site or fewer than 3 lymph nodes with at least 1 of them measured ≥ 1 cm along the short axis or spherical form or central necrosis. The anatomical criteria for lung metastasis included solid pulmonary nodules, reticulonodular pattern, cavitating nodules, or a lymphangitis carcinomatosis. The anatomical criteria for bone metastasis were lytic or sclerotic lesions with cortical breakthrough, periosteal reaction, expansile appearance, or pathological fracture observed by CT or an abnormal marrow signal intensity observed on MRI. The anatomical criteria for distant metastasis included a nodule or mass lesion at another site. Lesions showing focal increased tracer uptake beyond the background and corresponding

anatomical criteria were defined as true positives. Patients with negative PET/CT findings were followed up clinically for at least 3 months to confirm a true negative result.

Statistical Analysis

The primary outcome was concordance of FDG and FAPI PET/CT for initial staging and recurrence detection. The secondary outcome was diagnostic accuracy of both tracers. The comparison of semiquantitative parameters was the tertiary outcome.

The visually interpreted PET/CT images were compared with the reference standards. Concordant rates between both tracers for initial staging and recurrence detection were calculated. Diagnostic accuracy of both tracers defined by sensitivity, specificity, positive predictive value (PPV), negative predictive value (NPV), and accuracy was calculated for lesions with histopathological validation. Differences in semiquantitative parameters between ^{18}F-FDG and ^{68}Ga-FAPI-46 PET/CT were analyzed using paired t-tests. Data are presented as numbers or means ± standard deviations. A P value of < 0.05 was considered statistically significant. STATA software, version 11 (StataCorp LLC; College Station, TX, USA) was applied for all analyses.

RESULTS

Characteristics of each patient were shown in Table 1.

Twenty-five primary tumors were detected in 25 patients using both tracers. The mean size of the primary tumors was 3.5±1.4 cm with a minimum and maximum of 1.5 cm and 7.4 cm, respectively.

^{18}F-FDG and ^{68}Ga-FAPI-46 identified 128 and 94 lymph nodes, respectively. Overall, there were 33 sites (17 neck, 5 supraclavicular, 1 axilla, 7 mediastinum, and 3 intra-abdomen) of nodal involvement in 24 patients detected by both tracers. The ^{18}F-FDG PET/CT detected more lymph nodes than ^{68}Ga-FAPI-46 PET/CT; however, the numbers of sites involved were not different

between the 2 tracers. The sizes of detected nodes ranged from 0.4 cm to 4.2 cm. Patient with lower nodal detection by the ^{68}Ga-FAPI-46 tracer was shown in Figure 2.

Ten of 40 patients presented with distant metastasis involving 15 sites (5 lung, 5 bone, 1, pleura,1 thyroid, 1 adrenal gland, 1 liver, 1 muscle). Synchronous tumors were noted in 4 patients (supraglottis in 1 patient and esophagus in 3 patients). Two patients had second primary thyroid cancer with histopathological confirmation. The lesions at each site were detected with both tracers, except for two bone lesions in 2 patients which were observed only by ^{68}Ga-FAPI-46. Both bone lesions were confirmed by anatomical criteria for bone metastasis.

Concordance of FDG and FAPI PET/CT

There was no difference in the assessment of TNM staging between the two tracers in 10 of 12 patients, with 83.3% concordance. ^{68}Ga-FAPI-46 PET/CT upstaged 1 patient (patient number 28). The upstaged lesion was confirmed with an MRI following a marrow change at the right scapula and suspected bone metastasis. In patient number 31, ^{68}Ga-FAPI-46 PET/CT detected a lower number of nodal metastases than ^{18}F-FDG. In this latter case, the nodal metastases were confirmed by anatomical criteria as the sizes of discordant node were 1.0 cm and 1.2 cm in short axis and long axis, respectively. Details of the PET/CT results for initial staging were shown in Table 2.

A difference in recurrence detection between the 2 tracers was observed only in 1 of 28 patients, with 96.4% concordance. In this case, ^{68}Ga-FAPI-46 PET/CT showed focal uptake without a corresponding ^{18}F-FDG uptake in a sclerotic lesion at the 9th right rib, which was suspected bone metastasis according to our criteria. Images of the discordant cases were presented in Figure 3. False positive result in patient number 1 may be explained by post-operative inflammation due to primary tumor excision about 1 month before PET studies. False positive result with a biopsy validation in patient number 14 may be clarified by post-radiation fibrotic

change at 5 months after radiation. Details of the PET/CT results for recurrence detection were shown in Table 3.

Diagnostic Accuracy of FDG and FAPI PET/CT

Eighteen lesions had histopathological results. Both tracers detected 16 true positive, 1 true negative, and 1 false positive lesion. No false negative results were reported. Diagnostic accuracy of FAPI and FDG PET/CT was shown in Table 4.

Comparison of the Semiquantitative Parameters

There was no significant difference in semiquantitative parameters, except FTV of primary tumor which was significantly higher than MTV ($P = 0.03$). An example of a patient with higher FTV than MTV was demonstrated in Figure 4. The semiquantitative comparisons of primary tumor and distant metastasis were shown in Table 5. The semiquantitative parameter comparisons of nodal metastasis were presented in Table 6.

DISCUSSION

This is the first study of a head-to-head comparison of diagnostic performance and semiquantitative parameters, such as uptake, image contrast, and tumor volume, between ^{68}Ga-FAPI-46 and ^{18}F-FDG PET/CT in patients with HNSCC. We found that ^{68}Ga-FAPI-46 PET/CT had an 83.3% and 96.4% concordance rate with ^{18}F-FDG PET/CT for initial staging and recurrence detection, respectively. Lesion-based analysis showed comparable diagnostic accuracy. All primary tumors were detected by both tracers. We found that the number of avid nodes detected with ^{68}Ga-FAPI-46 was less than that detected with ^{18}F-FDG. Our study corresponded with Serfling et al. (*10*) who reported ^{18}F-FDG PET/CT detection rate for cervical nodal metastases was higher than that of ^{68}Ga-FAPI PET/CT, if the metastatic nodes were smaller than 0.7 cm; smaller nodes resulted in weaker FAP expression and delayed conversion of normal fibroblasts to CAFs. However, FAPI may have higher tumor specificity than FDG, which may

result in less false positive uptake in inflamed or otherwise reactive lymph nodes. Differences in detection of avid nodes will require further verification. Our study was discordant with Chen et al. (*5*) who observed higher sensitivity and lower specificity for nodal metastatic detection by ^{68}Ga-FAPI-04 compared with ^{18}F-FDG PET/CT. However, Chen et al. compared ^{68}Ga-FAPI with ^{18}F-FDG PET/CT in various types of cancer with only 6 HNSCC patients. In our study, ^{68}Ga-FAPI-46 and ^{18}F-FDG PET/CT showed consistency for detection of distant metastases in most cases. However, we observed detection differences in two bone lesions that showed ^{68}Ga-FAPI-46 avidity but no ^{18}F-FDG uptake. Chen et al. (*5*) reported a false positive ^{68}Ga-FAPI avid bone lesion because of myelofibrosis, which was not observed with FDG. In the case that histopathological confirmation is not practical, multimodal imaging is required for morphological details of metastasis.

Compared with ^{18}F-FDG PET/CT, ^{68}Ga-FAPI-46 PET/CT showed higher contrast images with lower physiological background in the brain, salivary glands, and Waldeyer's ring. However, we found no significant differences between the 2 tracers for SUVmax, SUVmean, T/B, or TLG vs. TLF in the primary tumors. No significant differences in these semiquantitative parameters were observed between the tracers for nodal and distant metastases. Although there may be some variation in methods for SUV measurements, our results were consistent with the study of Ballal et al. (*11*) who demonstrated that patients with head and neck cancer had comparably high uptake of ^{68}Ga-DOTA.SA-FAPI and ^{18}F-FDG. Our study was not in agreement with Pang et al. (*12*) who observed higher uptake of ^{68}Ga-FAPI than ^{18}F-FDG in primary and metastatic lesions of patients with gastric, duodenal, and colorectal cancers. This may be explained by differences in glucose metabolism among various tumor cell types. Pang et al. studied patients with adenocarcinoma or signet-ring cell carcinoma. Greater than 50% of their subjects were gastric cancer patients, who showed low-to-moderate ^{18}F-FDG avidity, while our study recruited patients with HNSCC who usually demonstrated high ^{18}F-FDG uptake.

Interestingly, we observed a significantly higher FTV than MTV for the primary HNSCC tumor. Syed et al. (*6*) used ^{68}Ga-FAPI PET/CT to contour head and neck cancer and found that FAPI-based gross tumor volume was significantly different from CT-based gross tumor volume. When FAPI- and CT-based gross tumor volumes were merged using SUVmax thresholds of three-fold (20-25% SUVmax) and five-fold (40-50% SUVmax), the derived tumor volumes were significantly larger than that of CT-base volumes. We suggest that ^{68}Ga-FAPI-46–derived FTV may be an important semiquantitative parameter for HNSCC and will require further standardization and validation.

We found that sensitivity, specificity, PPV, NPV, and accuracy of both tracers were 100%, 50%, 94.1%, 100% and 94.4%, respectively. The 8 cases with negative ^{68}Ga-FAPI-46 and ^{18}F-FDG PET/CT findings had no histopathological confirmation, resulting in low true negative results and poor specificity in our study.

Our study was limited by the lack of histopathological confirmation. Using a fixed threshold of 40% of SUVmax was dependent on the signal-to-noise ratio, T/B and the size of the tumor. Adaptive threshold-based method or taking the background in consideration may be more suitable for tumor delineation. Precise definition of FTV is needs for further study. Although there were some limitations in our study, we observed that the diagnostic performance of ^{68}Ga-FAPI-46 PET/CT was in good concordance with standard ^{18}F-FDG PET/CT molecular imaging.

CONCLUSION

Our study reveals that ^{68}Ga-FAPI-46 PET/CT has good concordance and comparable diagnostic performance with ^{18}F-FDG PET/CT for initial staging and recurrence detection in patients with HNSCC. The majority of semiquantitative parameters were comparable between the 2 tracers. However, ^{68}Ga-FAPI-46–derived FTV was higher than the MTV of ^{18}F-FDG. Therefore,

FTV may be a potential semiquantitative parameter for tumor volume of primary HNSCC and will require further standardization and validation.

Financial disclosure

The authors declare no potential conflicts of interest with respect to the research, authorship, and/or publication of this article.

Acknowledgements

We thank Supanida Mayurasakorn, MD, for performing the clinical data collection and Ms. Sunattee Kessung for editing the draft of manuscript. We are grateful to Sofie iTheranostics Inc. for providing the ^{68}Ga-FAPI-46 precursor.

Key Points

Question: May ^{68}Ga-FAPI-46 PET/CT compare favorably to ^{18}F-FDG PET/CT in HNSCC patients?

Pertinent findings: ^{68}Ga-FAPI-46 PET/CT was 83.3% and 96.4% concordant with ^{18}F-FDG PET/CT for initial staging and recurrence detection, respectively. Diagnostic accuracy of ^{68}Ga-FAPI-46 PET/CT was equivalent to ^{18}F-FDG PET/CT. ^{68}Ga-FAPI-46–derived FTV was higher than MTV assessed by ^{18}F-FDG, but the other semiquantitative parameters were comparable.

Implications for patient care: ^{68}Ga-FAPI-46 PET/CT shows comparable diagnostic performance compared with ^{18}F-FDG PET/CT in detecting primary and metastatic HNSCC.

References

1. Ferlay J, Colombet M, Soerjomataram I, et al. Estimating the global cancer incidence and mortality in 2018: GLOBOCAN sources and methods. *Int J Cancer*. 2019;144:1941-1953.
2. Hentschel M, Appold S, Schreiber A, et al. Serial FDG-PET on patients with head and neck cancer: implications for radiation therapy. *Int J Radiat Biol*. 2009;85:796–804.
3. Johnson DE, Burtness B, Leemans CR, Lui VWY, Bauman JE, Grandis JR. Head and neck squamous cell carcinoma. *Nat Rev Dis Primers*. 2020;6:92.
4. Kratochwil C, Flechsig P, Lindner T, et al. 68Ga-FAPI PET/CT: Tracer uptake in 28 different kinds of cancer. *J Nucl Med*. 2019;60:801-805.
5. Chen H, Pang Y, Wu J, et al. Comparison of [68Ga]Ga-DOTA-FAPI-04 and [18F] FDG PET/CT for the diagnosis of primary and metastatic lesions in patients with various types of cancer. *Eur J Nucl Med Mol Imaging*. 2020;47:1820-1832.
6. Syed M, Flechsig P, Liermann J, et al. Fibroblast activation protein inhibitor (FAPI) PET for diagnostics and advanced targeted radiotherapy in head and neck cancers. *Eur J Nucl Med Mol Imaging*. 2020;47:2836-2845.
7. Lindner T, Loktev A, Altmann A, et al. Development of quinoline-based theranostic ligands for the targeting of fibroblast activation protein. *J Nucl Med*. 2018;59:1415-1422.
8. Loktev A, Lindner T, Mier W, et al. A tumor-imaging method targeting cancer-associated fibroblasts. *J Nucl Med*. 2018;59:1423-1429.
9. Lydiatt WM, Patel SG, O'Sullivan B, et al. Head and neck cancers-major changes in the American Joint Committee on cancer eighth edition cancer staging manual. *CA Cancer J Clin*. 2017;67:122-137.
10. Serfling S, Zhi Y, Schirbel A, et al. Improved cancer detection in Waldeyer's tonsillar ring by 68Ga-FAPI PET/CT imaging. *Eur J Nucl Med Mol Imaging*. 2021;48:1178-1187.

11. Ballal S, Yadav MP, Moon ES, et al. Biodistribution, pharmacokinetics, dosimetry of [68Ga]Ga-DOTA.SA.FAPi, and the head-to-head comparison with [18F]F-FDG PET/CT in patients with various cancers. *Eur J Nucl Med Mol Imaging*. 2021;48:1915-1931.
12. Pang Y, Zhao L, Luo Z, et al. Comparison of 68Ga-FAPI and 18F-FDG uptake in gastric, duodenal, and colorectal cancers. *Radiology*. 2021;298:393–402.

Figures with legends

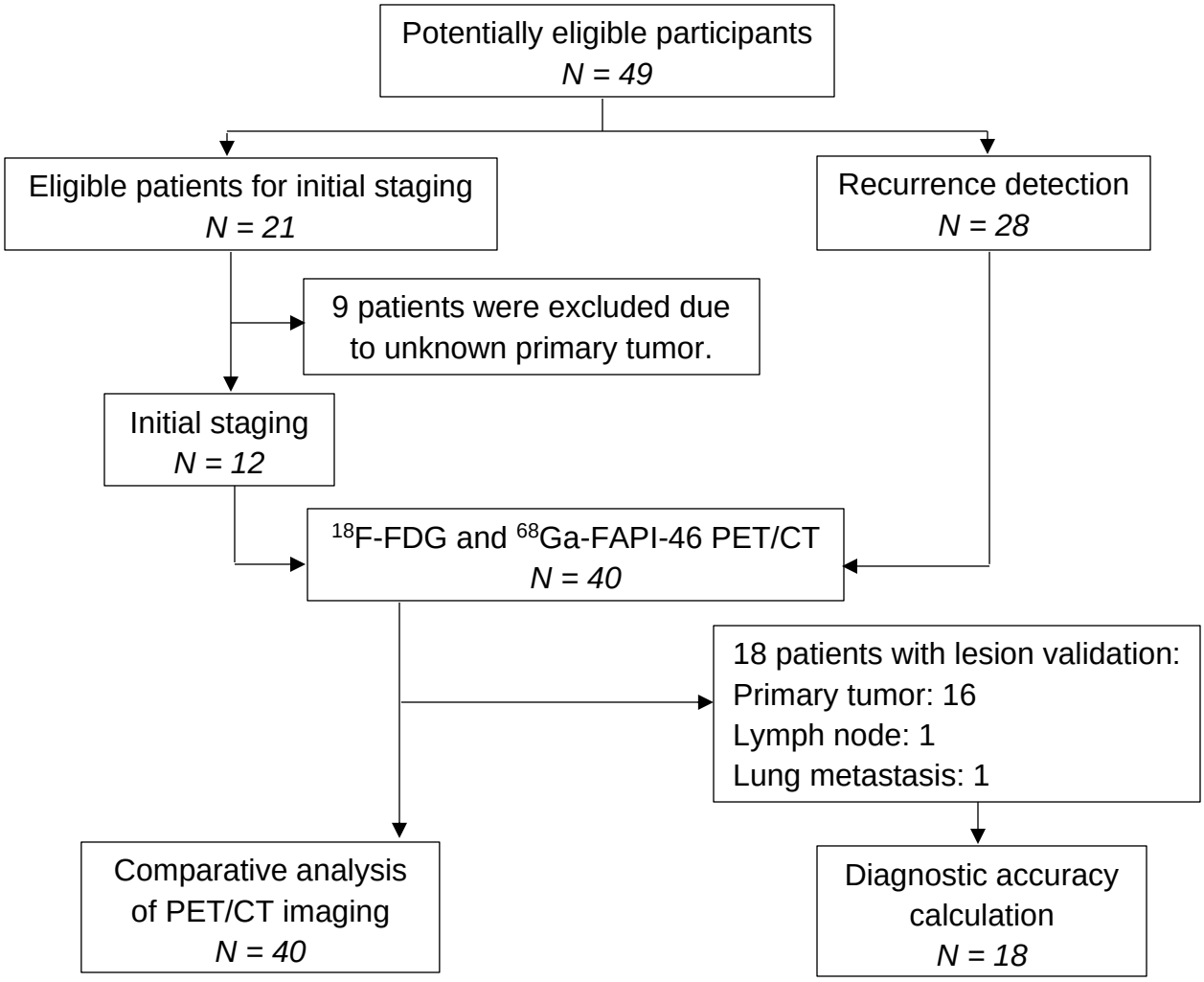

FIGURE 1. The flowchart of the study design

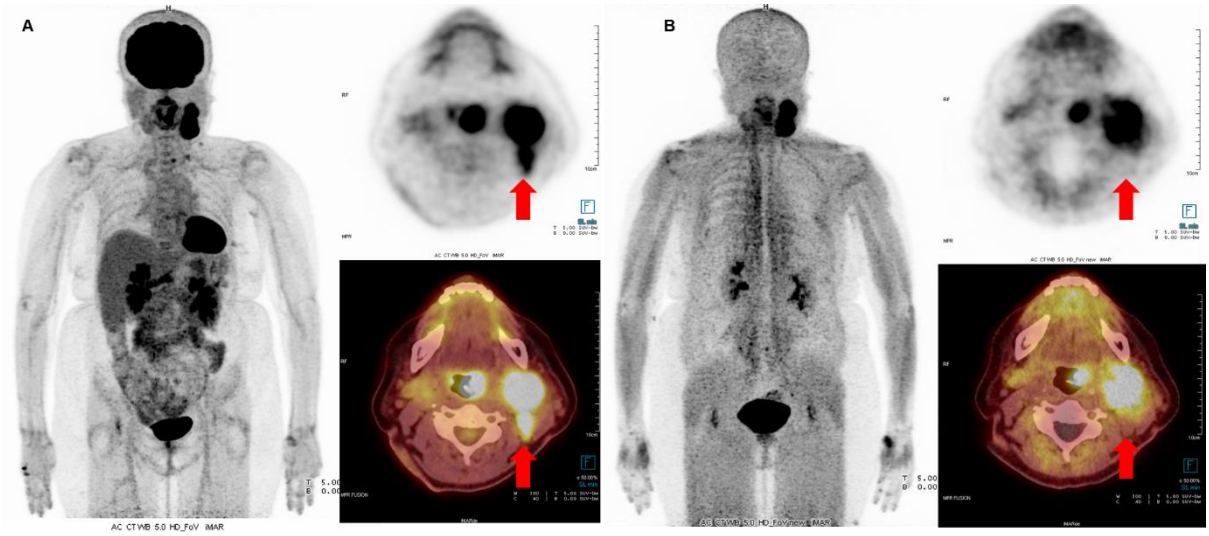

FIGURE 2. A: ^{18}F-FDG PET/CT; B: ^{68}Ga-FAPI-46 PET/CT. A 69-year-old woman with left oropharyngeal cancer, stage IVA, who underwent PET/CT for initial staging. ^{18}F-FDG PET/CT detected involved lymph nodes on the left side at levels IIA and IIB, while ^{68}Ga-FAPI-46 PET/CT did not detect the level IIB node (red arrow). The left IIB node was confirmed as a nodal metastasis by anatomical abnormality criteria.

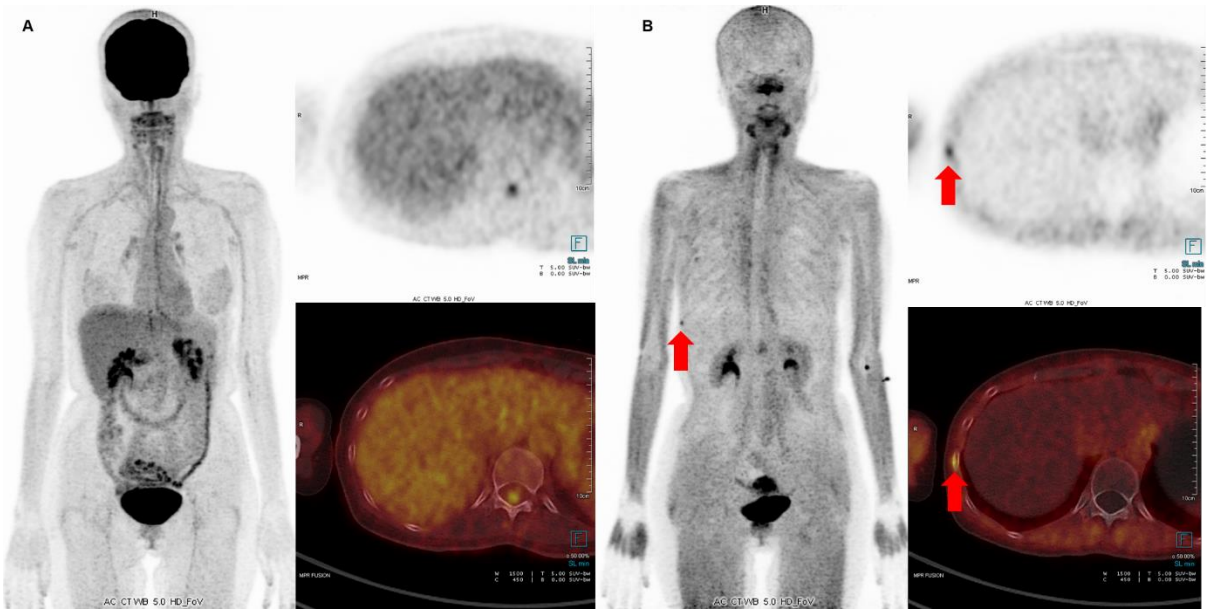

FIGURE 3. A: ^{18}F-FDG PET/CT; B: ^{68}Ga- FAPI-46 PET/CT. A 49-year-old female with nasopharyngeal cancer after concurrent chemoradiation who underwent PET/CT for recurrence detection. ^{68}Ga-FAPI-46 PET/CT showed focal uptake, without corresponding ^{18}F-FDG uptake, in a small sclerotic lesion at the 9th right lateral rib, which was suspected of being bone metastasis (red arrow).

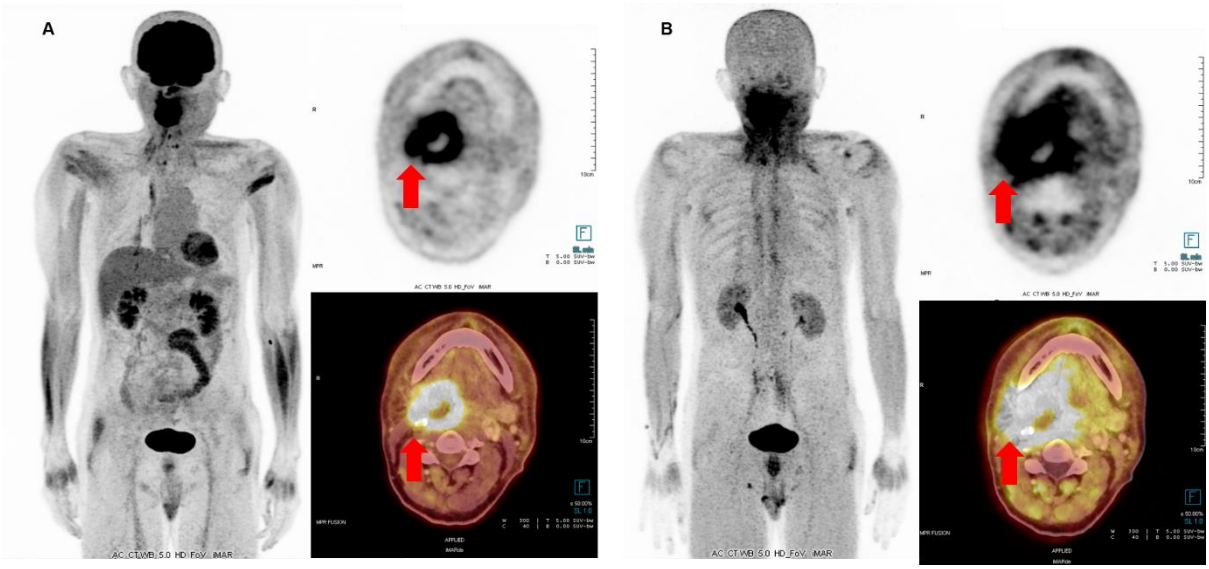

FIGURE 4. A: ^{18}F-FDG PET/CT; B: ^{68}Ga-FAPI-46 PET/CT. A 60-year-old man with glottic cancer who underwent PET/CT for recurrence detection. There was a ^{18}F-FDG and ^{68}Ga-FAPI-46 avid recurrent tumor at the right side of the oropharynx (red arrow). MTV was 19.37 cm^3. FTV was 33.75 cm^3.

Graphical abstract

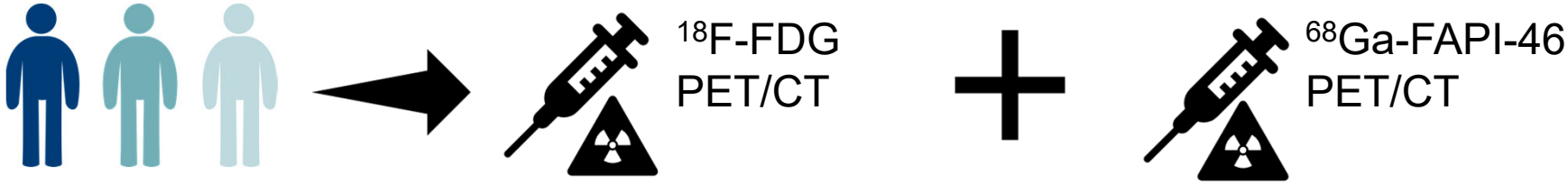

HNSCC patients with indication for initial staging or suspected recurrence.

Implications: ^{68}Ga-FAPI-46 PET/CT shows comparable diagnostic performance compared with ^{18}F-FDG PET/CT in detecting primary and metastatic HNSCC.

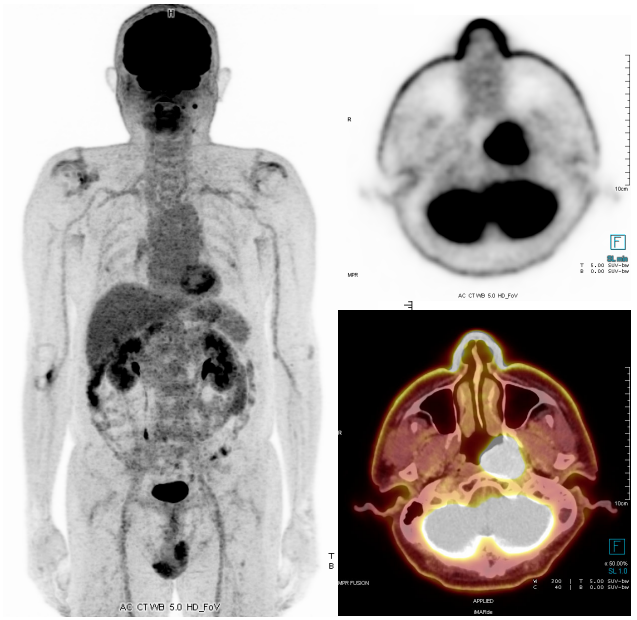

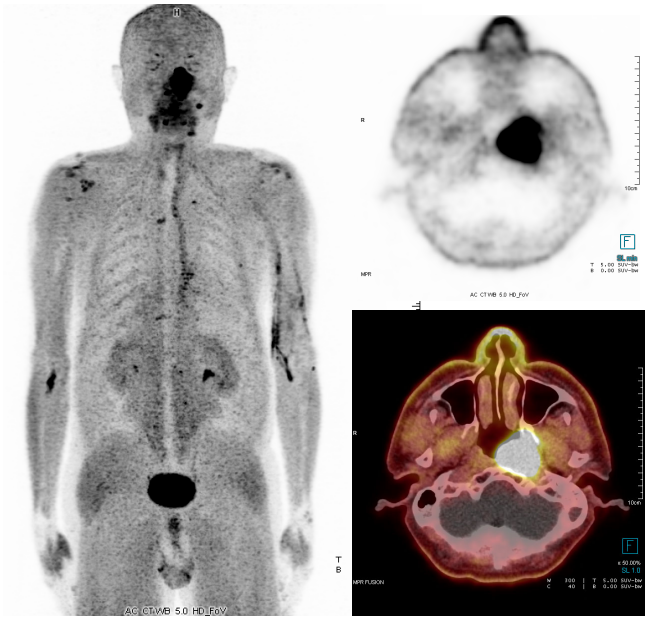

Tables

TABLE 1. Characteristics of the study patients

Patient No.	Age	Gender	Primary tumor	Indication
1	48	M	Tongue	Recurrence detection
2	65	F	Lip	Recurrence detection
3	65	M	Pyriform	Recurrence detection
4	57	M	Tongue	Recurrence detection
5	65	M	BOT	Initial staging
6	57	F	Nasopharynx	Recurrence detection
7	49	F	External ear canal	Recurrence detection
8	35	F	Nasal cavity	Recurrence detection
9	54	F	Nasopharynx	Recurrence detection
10	62	M	Nasopharynx	Recurrence detection
11	69	F	Oropharynx	Initial staging
12	62	F	Tongue	Initial staging
13	58	M	Pyriform	Initial staging
14	79	M	Tongue	Recurrence detection
15	67	M	Pyriform	Recurrence detection
16	77	M	Retromolar trigone	Recurrence detection
17	45	F	Oral mucosa	Initial staging
18	51	M	Nasopharynx	Initial staging
19	59	M	Nasopharynx	Initial staging
20	55	M	BOT	Recurrence detection
21	50	M	Tongue	Initial staging
22	32	F	Nasopharynx	Recurrence detection
23	60	M	BOT	Recurrence detection
24	60	M	Glottis	Recurrence detection
25	61	M	Pyriform	Recurrence detection
26	69	M	Nasopharynx	Recurrence detection
27	63	M	Floor of mouth	Recurrence detection
28	62	M	Pyriform	Initial staging
29	74	M	Nasopharynx	Recurrence detection
30	86	M	Nasopharynx	Recurrence detection
31	55	M	Nasopharynx	Initial staging
32	49	F	Nasopharynx	Recurrence detection
33	53	M	Nasopharynx	Recurrence detection
34	47	M	Nasopharynx	Recurrence detection
35	23	M	Nasopharynx	Recurrence detection
36	42	F	Tongue	Recurrence detection
37	46	M	Nasopharynx	Recurrence detection
38	32	F	Nasopharynx	Recurrence detection
39	51	M	Nasopharynx	Initial staging
40	72	F	Tongue	Initial staging

BOT: base of tongue; F: female; M: male; No.: number

TABLE 2. Comparative ^{18}F-FDG and ^{68}Ga-FAPI-46 PET/CT results for initial staging

Patient number	Primary tumor	TNM		Stage	
		^{18}F-FDG	^{68}Ga-FAPI-46	^{18}F-FDG	^{68}Ga-FAPI-46
5	Base of tongue	T2N2cM0	T2N2cM0	IVA	IVA
11	Oropharynx	T1N2bM0	T1N2bM0	IVA	IVA
12	Tongue	T3N2cM0	T3N2cM0	IVA	IVA
13	Pyriform	T1N3bM0	T1N3bM0	IVB	IVB
17	Oral mucosa	T3N1M0	T3N1M0	III	III
18	Nasopharynx	T3N2M0	T3N2M0	III	III
19	Nasopharynx	T3N1M0	T3N1M0	III	III
21	Tongue	T3N0M0	T3N0M0	III	III
28	Pyriform	T3N2bM0	T3N2bM1	IVA	IVC
31	Nasopharynx	T2N2M1	T2N1M1	IVB	IVB
39	Nasopharynx	T2N0M0	T2N0M0	II	II
40	Tongue	T2N0M0	T2N0M0	II	II

CT: computed tomography; ^{18}F-FDG:^{18}F-fluorodeoxy-D-glucose; ^{68}Ga-FAPI:^{68}Ga-fibroblast activation protein inhibitor; PET: positron emission tomography

TABLE 3. Comparative ^{18}F-FDG and ^{68}Ga-FAPI-46 PET/CT results for recurrence detection

Patient number	Primary tumor	Recurrence site	^{18}F-FDG avidity	^{68}Ga-FAPI-46 avidity	PET/CT result
1	Tongue	None	Y	Y	FP
2	Lip	Primary, LN	Y	Y	TP
3	Pyriform	Primary, LN	Y	Y	TP
4	Tongue	Primary, LN	Y	Y	TP
6	Nasopharynx	None	N	N	TN
7	External ear canal	Primary, LN	Y	Y	TP
8	Nasal cavity	None	N	N	TN
9	Nasopharynx	Primary	Y	Y	TP
10	Nasopharynx	Lung	Y	Y	TP
14	Tongue	None	Y	Y	FP
15	Pyriform	Primary	Y	Y	TP
16	Retromolar trigone	Primary, LN	Y	Y	TP
20	Base of tongue	Primary, LN, lung, thyroid	Y	Y	TP
22	Nasopharynx	LN, bone	Y	Y	TP
23	Base of tongue	None	N	N	TN
24	Glottis	Primary, LN	Y	Y	TP
25	Pyriform	LN, liver, adrenal gland	Y	Y	TP
26	Nasopharynx	Primary, LN, lung	Y	Y	TP
27	Floor of mouth	Primary, LN, bone, muscle	Y	Y	TP
29	Nasopharynx	None	N	N	TN
30	Nasopharynx	LN, lung	Y	Y	TP
32	Nasopharynx	Bone	N	Y	FN for FDG TP for FAPI
33	Nasopharynx	None	N	N	TN
34	Nasopharynx	LN, nasal turbinate	Y	Y	TP
35	Nasopharynx	None	N	N	TN
36	Tongue	None	N	N	TN
37	Nasopharynx	None	N	N	TN
38	Nasopharynx	LN, lung, pleura	Y	Y	TP

CT: computed tomography; ^{18}F-FDG:^{18}F-fluorodeoxy-D-glucose; ^{68}Ga-FAPI:^{68}Ga-fibroblast activation protein inhibitor; FN: false negative; FP: false positive; LN: lymph node; N: no; PET: positron emission tomography; TN: true negative; TP: true positive; Y: yes

TABLE 4. Comparative diagnostic accuracy of ^{18}F-FDG and ^{68}Ga-FAPI-46 PET/CT

Diagnostic accuracy (%)	**^{18}F-FDG**	**^{68}Ga-FAPI-46**
Sensitivity	100	100
Specificity	50	50
Positive predictive value	94.1	94.1
Negative predictive value	100	100
Accuracy	94.4	94.4

CT: computed tomography; ^{18}F-FDG:^{18}F-fluorodeoxy-D-glucose; ^{68}Ga-FAPI:^{68}Ga-fibroblast activation protein inhibitor; PET: positron emission tomography

TABLE 5. Comparisons of semiquantitative parameters between ^{18}F-FDG and ^{68}Ga-FAPI-46 PET/CT of primary tumor and distant metastasis.

Parameter	^{18}F-FDG	^{68}Ga-FAPI-46	P value
Primary tumor			
- SUVmax	18.59±9.61(7.15-43.11)	19.28±7.45(6.40-42.39)	0.65
- SUVmean	10.82±6.10(2.54-24.64)	11.10±4.83(4.17-28.07)	0.78
- T/B	10.21±5.89(1.54-26.37)	11.04±5.03(2.21-23.51)	0.45
- MTV vs FTV	7.36±5.07(1.34-21.66)	10.33±9.44(0.86-35.37)	0.03
- TLG vs TLF	94.91±117.20(7.14-517.65)	122.58±132.85(8.88-500.50)	0.06
Distant metastasis			
- SUVmax	13.59±7.64(3.86-31.69)	16.89±9.96(3.09-34.22)	0.09
- SUVmean	7.82±4.45(2.23-18.42)	9.74±5.67(1.80-18.18)	0.09
- T/B	30.39±55.85(1.53-254.4)	20.54±13.57(1.69-52.63)	0.44
- MTV vs FTV	10.52±19.41(0.18-81.23)	9.02±15.27(0.25-54.42)	0.33
- TLG vs TLF	109.87±255.52(1.43-1151.59)	135.92±260.12(0.78-976.03)	0.36

The data are presented as means ± standard deviations (minimum–maximum).

CT: computed tomography; ^{18}F-FDG: ^{18}F-fluorodeoxy-D-glucose; FTV: FAP expression tumor volume (^{68}Ga-FAPI); ^{68}Ga-FAPI: ^{68}Ga-fibroblast activation protein inhibitor; MTV: metabolic tumor volume (^{18}F-FDG); PET: positron emission tomography; SUVmax: maximum standardized uptake value; SUVmean: mean standardized uptake value; T/B: tumor-to-background ratio; TLF: total lesion FAP expression (^{68}Ga-FAPI); TLG: total lesion glycolysis (^{18}F-FDG)

TABLE 6. Semiquantitative comparisons between ^{18}F-FDG and ^{68}Ga-FAPI-46 PET/CT for nodal metastasis

Sites	Median size (cm)	Number of detected nodes		SUVmax*		P value†
		^{18}F-FDG	^{68}Ga-FAPI-46	^{18}F-FDG	^{68}Ga-FAPI-46	
Neck	1.3	85	56	13.67±7.38	16.91±9.35	0.08
Supraclavicular	0.8	5	4	9.97±3.47	7.16±2.01	
Mediastinum	0.8	30	22	9.21±4.22	8.64±4.54	
Axilla	1.1	3	3	18.64	10.98	
Intra-abdomen	0.9	5	9	15.83±7.02	31.84±9.00	
All	1.1	128	94	12.55±6.68	15.04±10.25	

* The data are presented as means ± standard deviations (minimum–maximum).

† P value of SUVmax

CT: computed tomography; ^{18}F-FDG:^{18}F-fluorodeoxy-D-glucose; ^{68}Ga-FAPI:^{68}Ga-fibroblast activation protein inhibitor; PET: positron emission tomography

Study protocol

1. Title: Head-to-head comparison of ^{68}Ga-FAPI-46 and ^{18}F-FDG PET/CT for evaluation of head and neck squamous cell carcinoma: a single-center exploratory study
2. Objective: A head-to-head comparison of the performance of ^{68}Ga-FAPI-46 PET/CT and standard ^{18}F-FDG PET/CT imaging for detecting primary cancer and metastatic lesions in patients with head and neck squamous cell carcinoma.
3. Outcome

   3.1 Primary outcome: Concordance of FAPI and FDG PET/CT

   3.2 Secondary outcome: Diagnostic accuracy of FAPI and FDG PET/CT

   3.3 Tertiary outcome: Comparison of semiquantitative parameters
4. Study design: Observational study
5. Study population: Patients with pathologically confirmed head and neck squamous cell carcinoma who were referred for PET scan with indication for initial staging or suspected recurrence.
6. Inclusion criteria

   6.1 Patients with pathologically confirmed head and neck squamous cell carcinoma

   6.2 Patients who were > 18 years old.

   6.3 Patients who were scheduled for PET/CT with indication for initial staging or suspected recurrence.
7. Exclusion criteria

   7.1 Patients with fasting blood sugar > 150 mg/dL

   7.2 Patients who were pregnant or breast feeding.

   7.3 Patients who were unwilling to participate.

8. Study procedure

8.1 Patient was scheduled ^{18}F-FDG PET/CT and ^{68}Ga-FAPI-46 PET/CT within 2 weeks apart

8.2 ^{18}F-FDG PET/CT day

8.2.1 Patient fasted for 6 h prior

8.2.2 Plasma glucose level was determined to ensure it is ≤ 150 mg/dL.

8.2.3 Patient had 2.59 MBq/kg of ^{18}F-FDG intravenous injection, uptake time 60 min

8.2.4 PET/CT acquired from the vertex to the proximal thigh (with arms in the down-position) using a 64-slice Siemens/Biograph vision PET/CT scanner (Siemens Healthcare GmbH, Erlangen, Germany) in the three-dimensional mode. The continuous bed motion method with a speed of 1.6–1.8 mm/s. The matrix size 440 x 440.

8.2.5 Reconstruction methods: True X and Time of Flight (Ultra HD PET).

8.2.6 CT parameters: tube voltage of 120 kV, current of 25 mAs with Siemens CARE Dose technology, and a slice thickness of 3.0 mm.

8.3 ^{68}Ga-FAPI-46 PET/CT day

8.3.1 No specific patient preparation

8.3.2 Patient had 2.0 MBq/kg of ^{68}Ga-FAPI-46 intravenous injection, uptake time 60 min

8.3.3 PET/CT acquisition, reconstruction and CT parameter as ^{18}F-FDG PET/CT

8.4 PET/CT analysis

8.4.1 ^{18}F-FDG and ^{68}Ga-FAPI-46 PET/CT scans were separately interpreted by three board-certified nuclear medicine physicians who were unaware of the clinical data or histopathological results at the time of review.

8.4.2 An area of focal tracer uptake higher than that of the surrounding background was considered positive by visual analysis. The lesion was categorized as a primary tumor, involved lymph node or distant metastasis.

8.4.3 Three-dimensional voxels of interest were drawn around the lesions seen on visual analysis by using threshold of 40% of SUVmax. Semiquantitative analysis including SUVmax, SUVmean, tumor-to-background ratio, metabolic tumor volume, total lesion glycolysis, FAP expression tumor volume, total lesion FAP expression were calculated. Tumor-to-background ratio was determined by dividing SUVmax with SUVmean of the contralateral normal tissue.

8.5 Data analysis

8.5.1 Histopathology served as the gold standard for diagnostic accuracy calculation. For non-biopsied lesions, anatomical abnormality observed on CT or MRI was used as reference.

8.5.2 Anatomical abnormal criteria for non-biopsied lesion as the follow;

8.5.2.1 Nodal metastasis: a cluster of at least 3 size-independent nodes were present at one site or if fewer than 3 lymph nodes were present and at least 1 of them measured ≥ 1 cm along the short axis or spherical form or showed central necrosis.

8.5.2.2 Lung metastasis: solid pulmonary nodules, nodules with a reticulonodular pattern, cavitating nodules, or a lymphangitis carcinomatosis pattern.

8.5.2.3 Bone metastasis: lytic or sclerotic lesions with cortical breakthrough, periosteal reaction, expansile appearance, or pathological fracture observed by CT scan or an abnormal marrow signal intensity observed on MRI.

8.5.2.4 Distant metastasis at another site: a nodule or mass forming lesion

8.5.3 Lesions showing a focal increased tracer uptake beyond the background and corresponding anatomical abnormality criteria were defined as true positives. Patients with negative PET/CT findings were followed up clinically for at least 3 months to confirm a true negative result.

8.5.4 For initial staging, the clinical TNM stage of head and neck squamous cell carcinoma was based on the eighth edition of the American Joint Committee on Cancer staging system.

8.6 Statistical analysis

8.6.1 Concordant rates between ^{18}F-FDG PET/CT and ^{68}Ga-FAPI-46 PET/CT for initial staging and recurrence detection. For initial staging, concordance is the agreement of PET/CT results in all T and N and M staging. For recurrence detection, concordance is the agreement of PET/CT studies in detecting recurrent lesions, either positive or negative results.

8.6.2 Diagnostic accuracy of ^{18}F-FDG PET/CT and ^{68}Ga-FAPI-46 PET/CT defined by sensitivity, specificity, positive predictive value, negative predictive value, and accuracy.

8.6.3 Differences in semiquantitative parameters between ^{18}F-FDG and ^{68}Ga-FAPI-46 PET/CT were analyzed using paired t-tests.

8.6.4 A P value of < 0.05 was considered statistically significant.